Photoaffinity Labeling of Human Sex Hormone-Binding Globulin Using 17α-Alkylamine Derivatives of 3β-Androstanediol Substituted with Azidonitrophenylamido, Azidonitrophenylamino, or Trifluoroazidonitrophenylamino Chromophores. Localization of Trp-84 in the Vicinity of the Steroid-Binding Site†

Christophe Chambon,‡ Djamila Bennat,‡ Frédéric Delolme,§ Guy Dessalces,§ Thierry Blachère,‡ Marc Rolland de Ravel,‡ Elisabeth Mappus,‡ Catherine Grenot,‡ and Claude Y. Cuilleron*,‡

Institut National de la Santé et de la Recherche Médicale, Unité INSERM U 329, Pathologie Hormonale Moléculaire, Hôpital Debrousse, 69322 Lyon, France, and Service Central d'Analyse, SCA-CNRS-USR59, 69390 Vernaison, France

Received July 19, 2001; Revised Manuscript Received September 24, 2001

ABSTRACT: Purified human SHBG was photoaffinity labeled with 17α-aminomethyl (M), 17α-aminoethyl (E), and 17α-aminopropyl (P) derivatives of [3α-^{3}H]-5α-androstane-3β,17β-diol coupled to 5-azido-2-nitrobenzoylamido (ANB), 4-azido-2-nitrophenylamino (ANP), and 5-azido-2-nitro-3,4,6-trifluorophenylamino (ANTFP) chromophores. Successful labeling was achieved in all cases except for the two photoreagents with the shortest side chains, namely, ANP-M and ANTFP-M derivatives. Edman sequencing and mass spectrometry of immunopurified photolabeled tryptic fragments revealed that radioactivity was present either on the sequence of residues 73−94, uniquely at the level of Trp-84 (stable covalent labeling), or on one of the two overlapping sequences of residues 126−134 and 126−135, at the level of Pro-130 (labile labeling) and Lys-134 (either stable or partially labile labeling), respectively. The same Trp-84 was photolabeled with the three ANB derivatives of increasing lengths, and by the ANP-P photoreagent. This residue was the exclusive target for the shortest [^{3}H]ANB-M photoreagent but was a minor site for the longest [^{3}H]ANB-P photoreagent, essentially recovered at the level of Pro-130. The [^{3}H]ANB-E photoreagent of intermediate size also labeled exclusively Trp-84, except in some experiments in which photolabeling was recovered predominantly at the level of Pro-130. The [^{3}H]ANP-P photoreagent with an overall length similar to that of the ANB-P photoreagent labeled simultaneously Trp-84 (minor site) and Lys-134. The other [^{3}H]ANP-E, [^{3}H]ANTFP-E, and [^{3}H]ANTFP-P derivatives labeled in all cases Lys-134. These findings indicate that the conserved Trp-84 and the two Pro-130 and Lys-134 residues are all located in the vicinity of the D ring of steroid ligands and remain freely accessible from the C17α position, thus providing biochemical data delineating the corresponding region of the steroid-binding site.

Human sex hormone-binding globulin (SHBG),[1] also called sex steroid-binding protein (SBP), is a plasma homodimeric glycoprotein mainly known to transport active steroids to target cells and to regulate their bioavailability (*1*, *2*). Human SHBG binds androgens (5α-dihydrotestosterone and testosterone) with high affinity and estrogens (estradiol) with a lower affinity (*3*), which can be further reduced in the presence of zinc (*4*).

Photoaffinity labeling experiments of human, rabbit, and sheep SHBGs with the unsubstituted androgenic Δ^6-testosterone reagent and of human SHBG with the corresponding estrogenic Δ^6-estradiol derivative have demonstrated that, in all cases, the conserved Met-139 residue is the unique site of photolabeling (*5*−*7*). The location of a part of the binding site around Met-139 is in agreement with the results of other affinity labeling studies that revealed additional labeled sites in this region, such as Lys-134 of human SHBG, alkylated with the 17β-bromoacetoxy derivative of [^{14}C]DHT (*8*), or the peptidic fragment between Ile-141 and Ser-151 of rat ABP, photoaffinity labeled with Δ^6-testosterone (*9*). Site-directed mutagenesis experiments have unambiguously confirmed the importance of Met-139 (*10*−*12*) and of the region of residues 130−138 (*13*, *14*) for the steroid binding properties of SHBG and, more recently, have also demonstrated the importance of Tyr-57 and Met-107 for the binding of ring A of DHT, but not of estradiol (*15*). The photoaffinity labeling of Met-139 with Δ^6-testosterone or Δ^6-estradiol derivatives suggests that Met-139 is close to the C3−C7 side

† This work was supported by the Institut National de la Santé et de la Recherche Médicale (INSERM).

* To whom correspondence should be addressed. Telephone: (33) 4 78 25 18 08. Fax: (33) 4 78 25 61 68. E-mail: cuilleron@lyon151.inserm.fr.

‡ Unité INSERM U 329.

§ SCA-CNRS-USR59.

[1] Abbreviations: ABP, androgen-binding protein; ANB-M/E/P, 17α-{[(5-azido-2-nitrobenzoyl)amido]methyl/ethyl/propyl}-5α-androstane-3β,17β-diol; ANP-M/E/P, 17α-{[(4-azido-2-nitrophenyl)amino]methyl/ethyl/propyl}-5α-androstane-3β,17β-diol; ANTFP-M/E/P, 17α-{[(5-azido-2-nitro-3,4,6-trifluorophenyl)amino]methyl/ethyl/propyl}-5α-androstane-3β,17β-diol; DHT, 5α-dihydrotestosterone; HPLC, high-performance liquid chromatography; MALDI-TOF-MS, matrix-assisted laser desorption/ionization time-of-flight mass spectrometry; $NaDodSO_4$, sodium dodecyl sulfate; PTH, phenylthiohydantoin; PBS, phosphate-buffered saline; PSD, post-source decay; SHBG, sex hormone-binding globulin; TLC, thin-layer chromatography; TFA, trifluoroacetic acid; Tris-HCl, tris(hydroxymethyl)aminomethane hydrochloride.

10.1021/bi011504s CCC: $20.00
Published on Web 11/17/2001

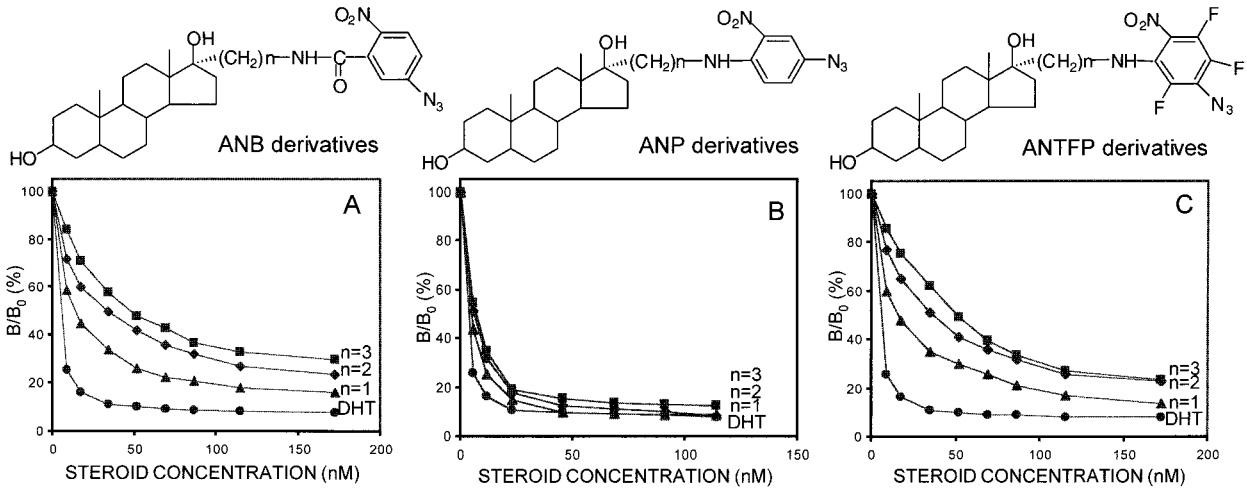

FIGURE 1: Competitive binding assays for DHT and the nine photoreagents with purified SHBG. Aliquots (100 μL) of purified SHBG (2.0 nM in PBS-gelatin) were incubated with 100 μL of [^{3}H]DHT (50 000 cpm, 0.45 nM in PBS-gelatin) and seven concentrations (ranging from 0 to 114 nM for the ANP photoreagents and from 0 to 172.5 nM for the ANB and ANTFP photoreagents) of each of the radioinert competitors in 100 μL of PBS-gelatin for 1 h at 22 °C and for 15 min at 4 °C. Free and bound steroids were separated by dextran-coated charcoal. For each competitor concentration, the radioactivity of bound [^{3}H]DHT (B) is expressed as the percentage of radioactivity bound in the absence of competitor (B_0): DHT (●), methyl ($n = 1$) intermediate linker (▲), ethyl ($n = 2$) intermediate linker (◆), and propyl ($n = 3$) intermediate linker (■) and ANB photoreagents (A), ANP photoreagents (B), and ANTFP photoreagents (C).

of the steroid ligand, whereas the chemoaffinity labeling of Lys-134 with 17β-bromoacetoxy DHT indicates that this residue should be in the proximity of the 17β-OH group. The observation that the homologous Asn-134 of sheep SHBG is contiguous to the glycosylated Asn-133 presumably located near the surface of the protein (*7*) and the efficiency of immobilized 17α-substituted 17β-hydroxysteroid derivatives as ligands for affinity chromatography purification of SHBG (*16*, *17*) have suggested a model of binding site in which the D ring of the steroid is oriented toward the surface of the protein, whereas the A and B rings are probably more buried in a hydrophobic region (*7*). All these findings proved to be in agreement with the recent three-dimensional structure established at 1.55 Å resolution for the recombinant N-terminal domain spanning residues 1−205 of human SHBG (*18*), crystallized in the presence of DHT (*19*).

The work presented here was undertaken in the hope of characterizing amino acids in the region of SHBG encompassing the D ring of the steroid ligand using photoaffinity labeling experiments performed with 5-azido-2-nitrobenzoylamido (ANB), 4-azido-2-nitrophenylamino (ANP), and 5-azido-2-nitro-3,4,6-trifluorophenylamino (ANTFP) photoactivatable chromophores coupled to three 17α-aminomethyl, 17α-aminoethyl, and 17α-aminopropyl derivatives of 5α-androstane-3β,17β-diol, a known ligand of human SHBG having only a slightly lower affinity than DHT (*20*).

EXPERIMENTAL PROCEDURES

Chemicals. [1,2,4,5,6,7-$^3H_6$]DHT (126 Ci/mmol) and [^{3}H]-$NaBH_4$ (8 Ci/mmol) were from Amersham Corp. DHT was from Roussel-UCLAF (Paris, France). L-1-(Tosylamido)-2-phenylethyl chloromethyl ketone trypsin (TPCK-trypsin) was from Worthington. Pig pancreatic elastase was from Roche. Trisacryl GF 05 was purchased from Sepracor (Villeneuve-la-Garenne, France).

Buffers included PBS [0.01 M sodium phosphate buffer (pH 7.4) and 0.15 M NaCl], PBS-gelatin (PBS containing 0.1% gelatin and 0.1% NaN_3), and Tris-HCl buffers [0.1, 0.25, or 0.5 M tris(hydroxymethyl)aminomethane hydrochloride at pH 8.2 or 8.5].

Synthesis of Photoaffinity Labeling Reagents. The synthesis and structural characterization of the nine 17α-{[(5-azido-2-nitrobenzoyl)amido]methyl}-5α-androstane-3β,17β-diol (ANB-M), 17α-{[2-(5-azido-2-nitrobenzoyl)amido]ethyl}-5α-androstane-3β,17β-diol (ANB-E), 17α-{[3-(5-azido-2-nitrobenzoyl)amido]propyl}-5α-androstane-3β,17β-diol (ANB-P), 17α-{[(4-azido-2-nitrophenyl)amino]methyl}-5α-androstane-3β,17β-diol (ANP-M), 17α-{[2-(4-azido-2-nitrophenyl)-amino]ethyl}-5α-androstane-3β,17β-diol (ANP-E), 17α-{[3-(4-azido-2-nitrophenyl)amino]propyl}-5α-androstane-3β,-17β-diol (ANP-P), 17α-{[(5-azido-2-nitro-3,4,6-trifluorophenyl)amino]methyl}-5α-androstane-3β,17β-diol (ANTFP-M), 17α-{[2-(5-azido-2-nitro-3,4,6-trifluorophenyl)amino]ethyl}-5α-androstane-3β,17β-diol (ANTFP-E), and 17α-{[3-(5-azido-2-nitro-3,4,6-trifluorophenyl)amino]propyl}-5α-androstane-3β,17β-diol (ANTFP-P) photoreagents (cf. Figure 1) have been reported (*21*).

The corresponding radioactive 17α-substituted [3α-^{3}H]-5α-androstane-3β,17β-diol photoreagents (~2 Ci/mmol) were prepared by reduction of an ice-cooled solution of the 3-ketone precursors (4 μmol in 100 μL of methanol) with a solution of [^{3}H]$NaBH_4$ in methanol (100 μL, 5 mCi) under an argon atmosphere. After 1 h in the dark, the reaction was stopped by addition of 300 μL of acetone and the radioactive steroids were purified by reverse-phase HPLC on a C_{18} column (Nucleosil, 10 μm, 0.7 cm × 25 cm) with an aqueous acetonitrile gradient (from 40 to 100% acetonitrile over the course of 60 min). The purity of the radiolabeled steroids was controlled by reverse-phase HPLC on a C_{18} column (Nucleosil, 5 μm, 0.46 cm × 15 cm) with the same aqueous acetonitrile gradient. The radioactivity profiles, detected online with a Flo-one Packard radiodetector, showed a radiochemical purity of >95%. The radioactive photoreagents were stored in absolute ethanol in the dark at −20 °C.

Purification of SHBG. Human SHBG was isolated by immunopurification from pools of human sera according to a protocol described elsewhere (*6*).

Binding Measurements. The association constants of immunopurified SHBG with the three tritiated ANB photoreagents were determined by equilibrium dialysis using Scatchard plots analyzed by a computer program with a least-squares fit of the data. Aliquots (1 mL) of immunopurified SHBG (9 nM) in PBS-gelatin buffer were placed inside dialysis bags and dialyzed for 20 h at 25 °C against eight concentrations (ranging from 2 to 40 nM) of ^{3}H-labeled steroid photoreagents, placed outside the bag in 10 mL of PBS buffer. Relative binding affinities were measured according to a reported protocol (*6*, *7*).

Photoaffinity Labeling. The conditions of photoaffinity labeling were essentially those described elsewhere (*6*). Immunopurified SHBG was first incubated for 1 h at 22 °C and 15 min at 4 °C, under an argon atmosphere, in the dark, with the different steroid photoreagents and irradiated with a high-pressure mercury lamp (Hanovia, 450 W), under an argon atmosphere, at $\lambda > 300$ nm, using a 2 mm thick Pyrex filter (*22*). After irradiation, the dissociation of noncovalently bound steroids was performed by exclusion chromatography of the irradiation mixture on microcolumns (Trisacryl GF 05) equilibrated with 0.1 M Tris-HCl (pH 8.5) containing 25% acetonitrile.

The following stoichiometries were employed in the incubation step prior to irradiation. (1) In photoinactivation experiments, SHBG (1.1×10^{-12} mol) was incubated with each of the photoreagents (11×10^{-12} mol) in the absence or presence of 22×10^{-12} mol of DHT in 200 μL of PBS-gelatin buffer. (2) For covalent photoattachment of tritiated photoreagents analyzed via cleavage with CNBr, SHBG (0.2 nmol) was incubated with [^{3}H]ANB-M, [^{3}H]ANB-E, [^{3}H]-ANB-P, and [^{3}H]ANTFP-E (0.2 nmol) in the absence or presence of DHT (1 or 2 nmol) in 50 μL of PBS. (3) For the determination of HPLC profiles of tryptic digests, SHBG (1 nmol) was incubated with each of the ^{3}H-labeled photoreagents (1 nmol) in 100 μL of PBS, in the absence or presence of DHT (10 nmol). (4) For photoaffinity labeling experiments using scavengers, SHBG (1 nmol) was incubated with [^{3}H]ANB-M or [^{3}H]ANB-P (1 nmol) in 100 μL of PBS containing 15 mM glutathione or 4-aminobenzoate. (5) For control experiments involving heat denaturation, heat-denatured SHBG (1 nmol) was incubated with [^{3}H]ANB-M or [^{3}H]ANB-P (1 nmol) in 100 μL of PBS. (6) For amino acid sequence analysis, (a) SHBG (40 nmol) was incubated with [^{3}H]ANB-M, [^{3}H]ANB-E, [^{3}H]ANB-P, [^{3}H]ANP-E, or [^{3}H]ANP-P (40 nmol dissolved in 5 μL of ethanol) in 2.5 mL of PBS or (b) SHBG (100 nmol) was incubated with [^{3}H]ANTFP-E (100 nmol dissolved in 15 μL of ethanol) in 6.5 mL of PBS. (7) For molecular mass determinations, SHBG (200 nmol) was incubated with [^{3}H]ANB-M, [^{3}H]-ANB-E, [^{3}H]ANB-P, [^{3}H]ANP-E, or [^{3}H]ANP-P (200 nmol dissolved in 30 μL of ethanol) in 12 mL of PBS.

Hydrolysis of Photolabeled SHBG. Photolabeled SHBG was reduced with dithioerythritol and carboxymethylated with iodoacetic acid in 0.25 M Tris-HCl buffer (pH 8.5) containing 6 M guanidinium chloride. (1) For cleavage with CNBr, reduced and carboxymethylated SHBG (0.2 mg) was transferred in 70% formic acid by exclusion chromatography, treated with CNBr (4 mg) for 20 h under a nitrogen atmosphere in the dark at room temperature, and lyophilized. (2) For cleavage with trypsin, reduced and carboxymethylated SHBG was transferred in 0.5 M Tris-HCl buffer (pH 8.2) by exclusion chromatography and treated with trypsin (1% enzyme/SHBG ratio, w/w) for 24 h at 37 °C. (3) For subcleavage with elastase of the tryptic peptide photolabeled with [^{3}H]ANB-M, the HPLC fraction containing the purified radioactive tryptic peptide was dried under a nitrogen stream, dissolved in 200 μL of 0.1 M Tris-HCl buffer (pH 8.2), and treated with elastase (10% enzyme/peptide ratio, w/w) for 24 h at 37 °C.

Immunopurification of Radioactive Tryptic Peptides with Antisteroid Antibodies. Poorly specific rabbit antibodies raised against a 17α-(5′-carboxypentyl)testosterone hapten coupled to bovine serum albumin (J. Dupret and C. Y. Cuilleron, unpublished results) were selected for their high cross-reactivity (50−80%) with the 17α-substituted photoreagents and purified by affinity chromatography using a 17α-hemiglutaramidomethyltestosterone derivative immobilized on Sepharose, according to reported procedures (*23*). The immunoaffinity gel was prepared by coupling the purified antibodies to CNBr-activated Sepharose 4B and used as a suspension in the same volume of 0.1 M Tris-HCl buffer (pH 8.2). Trypsin hydrolysates of SHBG photolabeled with radioactive steroid photoreagents were incubated with the immunoaffinity gel (3×10^6 dpm/mL of gel suspension) for 24 h at 4 °C. After elution of the unretained fractions (containing less than 20% of the initial radioactivity), the gel was washed with Tris buffer until no radioactivity could be detected. The radioactive peptides were desorbed with a solution of 30% dioxane in water (*24*) and concentrated rapidly under vacuum in a Speed-Vac concentrator to eliminate most of the dioxane. The radioactive peptides eluted from the affinity column were further purified by reverse-phase HPLC on a C_{18} column using an aqueous acetonitrile gradient in the presence of 0.1% TFA.

NaDodSO$_4$ Gel Electrophoresis. Sodium dodecyl sulfate−polyacrylamide gel electrophoresis (16.5% acrylamide) of peptides obtained after CNBr cleavage was performed as described by Schägger and Von Jagow (*25*) in a vertical slab-gel apparatus. Radioactive photolabeled peptides were detected by fluorography, after treatment of the gel with 1 M sodium salicylate, using Kodak BIOMAX MR film. ^{14}C-labeled, methylated molecular mass markers (ovalbumin, carbonic anhydrase, trypsin inhibitor, lysozyme, aprotinin, insulin B, and insulin A) were purchased from Amersham.

Sequence Determinations. Edman sequencing of purified peptides was performed with a gas-phase sequencer equipped with an on-line phenylthiohydantoin (PTH) analyzer (Applied Biosystems, model 473 sequencer).

Mass Spectrometry. Electrospray mass spectrometry experiments were performed on a Hewlett-Packard 5989 mass spectrometer equipped with an atmospheric pressure electrospray ion source at a resolution of 1000 (50% valley). The peptides were injected in 60 μL of aqueous methanol containing 1% acetic acid at a flow rate of 2 μL/min. The capillary exit voltage was 170 V. The quadrupole was scanning from *m*/*z* 400 to 2000. MALDI-TOF mass spectra were recorded on a Voyager-DE STR mass spectrometer (nitrogen laser at 337 nm) in the linear or reflector mode as well as in the PSD mode, using an α-cyano-4-hydroxycinnamic acid matrix, a positive polarity, an accelerating voltage of 20 or 25 kV, an extraction delay time varying from 150 to 200 ns, and an appropriate acquisition mass range ($M <$ 5000) or fragment ion window (PSD). The peptide (1−4

Table 1: Covalent Attachment of Photoreagents to Purified Human SHBG (Photoinactivation and Photolabeling Experiments)

	ANB			ANP			ANTFP		
intermediate linker	photoinactivation[a] (%)	photolabeling, undissociated[b] (molar ratio)	photolabeling, corrected[c] (molar ratio)	photoinactivation[a] (%)	photolabeling, undissociated[b] (molar ratio)	photolabeling, corrected[c] (molar ratio)	photoinactivation[a] (%)	photolabeling, undissociated[b] (molar ratio)	photolabeling, corrected[c] (molar ratio)
M	11	0.23	0.12	2	0.08	0	1	0.05	0
E	17	0.26	0.15	10	0.18	0.11	9	0.15	0.07
P	20	0.38	0.23	19	0.38	0.23	12	0.18	0.09

[a] SHBG was incubated and irradiated for 13 min with radioinert photoreagents as described in Experimental Procedures. Noncovalently bound steroids were eliminated by treatment with dextran-coated charcoal (1 mL, 1 h at 20 °C). SHBG binding capacity was measured on aliquots of supernatants (50 μL) incubated with [^{3}H]DHT (50 000 cpm) for 1 h at 20 °C. Free and bound steroids were separated by dextran-coated charcoal. Specific photoinactivation corresponds to the difference between photoinactivation in the absence of DHT and photoinactivation in the presence of a 20-fold molar excess of DHT. [b] The level of covalent attachment of tritiated photoreagents to SHBG was estimated as the amount of radioactivity that eluted under the proteic peak of the second exclusion chromatography (see Experimental Procedures). The level of specific covalent attachment, expressed as moles of label per mole of SHBG, corresponds to the difference between the total level of covalent attachment (in the absence of DHT) and the nonspecific level of covalent attachment (in the presence of a 10-fold molar excess of DHT). [c] Specific labeling corrected by subtraction of residual unbound photolyzed photoreagents, estimated from the percentage of residual non-peptide-bound radioactivity measured in HPLC radioactivity profiles of tryptic digests (48, 43, and 40% for ANB-M, -E, and -P, respectively; ~90, 39, and 40% for ANP-M, -E, and -P, respectively; ~90, 50, and 50% for ANTFP-M, -E, and -P, respectively).

pmol, solubilized in a 1/1 acetonitrile/0.5% aqueous TFA mixture, after desalting) was spotted and dried on the sample supporting device. The *m*/*z* values are expressed in Th (Thomson) units and are estimated to be accurate to ±1 in the PSD mode. Calculated masses are expressed in daltons.

RESULTS

Characterization of the Binding of Photoreagents to Immunopurified Human SHBG. The association constants estimated for the binding to SHBG of [^{3}H]ANB-M (2.0×10^9 M^{-1}), of [^{3}H]ANB-E (1.0×10^9 M^{-1}), and of [^{3}H]ANB-P (1.1×10^9 M^{-1}) were close to those estimated for testosterone (1.6×10^9 M^{-1}) but slightly lower than those estimated for DHT (3.7×10^9 M^{-1}). The abscissa intercepts of the linear Scatchard plots were the same for the photoreagents and for DHT within experimental error, thus suggesting the binding of all these derivatives at the same site. The association constants of the [^{3}H]ANP and [^{3}H]-ANTFP photoreagents for SHBG binding could not be determined precisely by equilibrium dialysis, because of strong adsorption of radioactivity on the glass or plastic tubes during the 20 h of incubation needed to reach binding equilibrium.

Displacement experiments with [^{3}H]DHT bound to SHBG (Figure 1) by the nine nonradioactive photoreagents showed that the highest competitive effects were observed with the three ANP photoreagents (relative binding affinities ranging from 50 to 60%), whereas ANB and ANTFP photoreagents were less effective (relative binding affinities ranging from 7.5 to 23% with ANB derivatives and from 7.5 to 28% with ANTFP derivatives). In each series, the level of displacement of [^{3}H]DHT bound to SHBG was found to decrease when the length of the intermediate linker between the steroid and the chromophore was increased, as previously shown for ANB conjugates of the three 17α-aminomethyl, 17α-aminoethyl, and 17α-aminopropyl derivatives of DHT (*21*).

Time Course of Photolysis of Photoreagents. Photolysis of radioinert photoreagents at $\lambda > 300$ nm, using a 2 mm thick Pyrex filter (*22*), was followed by recording UV absorption spectra as a function of irradiation time. Photolysis of tritiated photoreagents was analyzed by reverse-phase HPLC monitored simultaneously by UV absorbance and by on-line detection of radioactivity. In all cases, more than 90% of the photoreagent had undergone photolysis in less than 3 min, the photolysis being almost complete by 6 min.

Kinetics of Photoinactivation. The extent of photoinactivation of SHBG by each radioinert photoreagent was measured after irradiation at $\lambda > 300$ nm of SHBG samples using a 10/1 steroid/protein molar ratio of radioinert photoreagent, in the absence of DHT (total inactivation) and in the presence of a 20-fold molar excess of DHT (nonspecific inactivation). Irradiation for 13 min of SHBG incubated with the different photoreagents led in most cases to significant specific inactivations ranging from 9% of the initial binding capacity of SHBG for [^{3}H]DHT in the case of ANTFP-E to 20% in the case of ANB-P, whereas the two shortest ANP-M and ANTFP-M photoreagents were almost totally inactive (Table 1). The use of shorter irradiation times showed that photoinactivation was almost complete after 5 min while irradiation up to 30 min was unable to increase the extent of specific inactivation. As previously shown (*6*), the binding capacity of SHBG was not altered after irradiation for 15 min in the presence of DHT, thus confirming the stability of SHBG during irradiation.

Kinetics of Covalent Photoattachment of Tritiated Photoreagents. The covalent attachment of radioactive photoreagents to SHBG was studied at $\lambda > 300$ nm, using a 1/1 steroid/protein molar ratio in the absence or presence of a 10-fold molar excess of DHT. After elimination of the noncovalently bound radioactivity by exclusion chromatography, as reported previously (*6*), the maximal levels of both total and specific (i.e., inhibited by an excess of DHT) photolabeling were observed after irradiation for 6 min, in all cases. The levels of photolabeling varied from 0.05 and 0.08 mol of label per mole of SHBG with the two shortest [^{3}H]ANTFP-M and [^{3}H]ANP-M photoreagents, respectively, to 0.38 mol of label per mole of SHBG with the two longest [^{3}H]ANB-P and [^{3}H]ANP-P derivatives (Table 1). These values, systematically higher than those predicted from the corresponding photoinactivation yields, are probably overestimated, due to incomplete dissociation of unbound radioactivity by the exclusion chromatography step which could not be significantly improved by adding organic solvents or nonionic detergents. Finally, the presence of residual noncovalently bound steroids could be unambiguously detected and quantified by reverse-phase HPLC after trypsin hydroly-

sis of photolabeled SHBG (vide infra). The corrected yields (Table 1), fully consistent with photoinactivation yields, showed that the two smallest amounts of photolabeling mentioned above for the two two shortest [^{3}H]ANTFP-M and [^{3}H]ANP-M photoreagents did not correspond to covalent labeling, whereas the relative order of yields with the seven other photoreagents was not modified.

Control experiments without irradiation showed a total absence of irreversibly bound radioactivity. On the other hand, no covalent labeling occurred after incubation with prephotolyzed ANB photoreagents, thus indicating the absence of long-lived electrophilic intermediates (*26*).

CNBr Cleavage of Photolabeled SHBG. SHBG photolabeled with the three [^{3}H]ANB-M, [^{3}H]ANB-E, and [^{3}H]-ANB-P derivatives, as well as with the [^{3}H]ANTFP-E photoreagent, was reduced, carboxymethylated, and treated with CNBr. The separation of CNBr peptides by Na-DodSO_4−polyacrylamide gel electrophoresis showed in all cases the presence of radioactivity mainly at the level of ~3 kDa peptides, which was not maintained after photolabeling in the presence of an excess of DHT. The covalent attachment of radioactive photoreagents to ~3 kDa peptide(s) suggests that the sites of specific photolabeling are located in the N-terminal region before Met-139, since only this region is predicted to generate CNBr peptides of molecular masses ranging from 3 to 4.5 kDa.

Trypsin Hydrolysis of Photolabeled SHBG and Radioactivity Profiles of HPLC Separations of Tryptic Digests. Photolabeled SHBG fractions recovered after exclusion chromatography were reduced, carboxymethylated, and digested with trypsin. The radioactivity profiles of HPLC separations of tryptic peptides of SHBG photolabeled with ANB photoreagents (Figure 2) showed the presence of three major peaks for [^{3}H]ANB-M, one of them (peak 2) including a shoulder (Figure 2A), of four major peaks for [^{3}H]-ANB-E, three of them (peaks 1−3) including a shoulder (Figure 2B), and of three major peaks for [^{3}H]ANB-P (Figure 2C). For these three ANB derivatives, only the more retained peak was not abolished after photolabeling in the presence of a 10-fold molar excess of DHT. In some of the photolabeling experiments performed in this study with [^{3}H]-ANB-E, the above-mentioned peaks 1−3 were almost undetectable, whereas a new major peak (peak 3′) emerged at a retention time slightly higher than that of peak 3 (Figure 2B). However, reliable conditions controlling the preferred access to peak 3′ could not be established. The radioactivity profile of tryptic peptides of SHBG photolabeled with [^{3}H]-ANP-M showed only very small radioactive peaks (Figure 3) which were not studied further. The radioactivity profiles of samples photolabeled with [^{3}H]ANP-E and [^{3}H]ANP-P were similar and exhibited three major radioactive peaks, including a double peak 3. In both cases, peak 1 could not be abolished by photolabeling in the presence of DHT in contrast to a more retained associated peak (more intense than peak 1 in Figure 3C), which was not studied further. The radioactivity profiles of tryptic peptides of SHBG photolabeled with [^{3}H]ANTFP-E and [^{3}H]ANTFP-P exhibited two major radioactive peaks (Figure 4). In both cases, only peaks 2 were abolished by photolabeling in the presence of DHT. On the other hand, very small radioactive peaks were obtained with the shorter [^{3}H]ANTFP-M photoreagent, with the exception of the less-retained peak, assigned to unbound radioactivity, as also observed with the homologous nonfluorinated [^{3}H]ANP-M photoreagent.

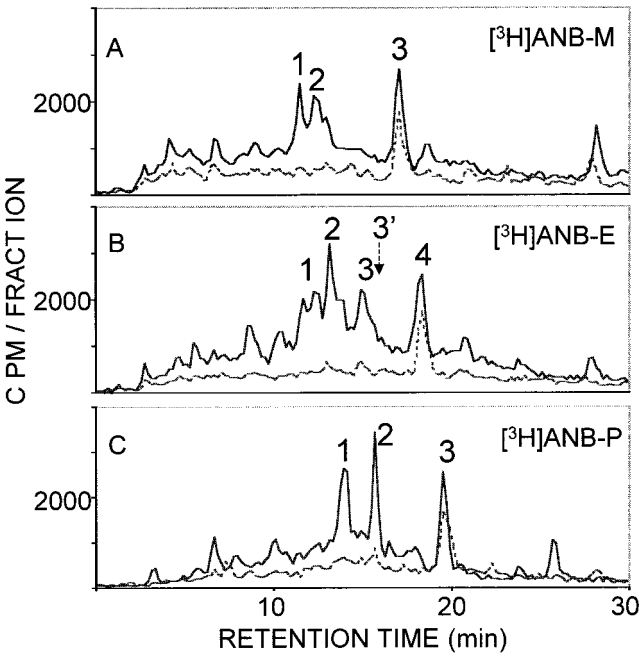

FIGURE 2: Reverse-phase HPLC separation of tryptic peptides of SHBG photolabeled with the [^{3}H]ANB photoreagents. The tryptic digests were applied on a C_{18} column (Nucleosil AB, 5 μm, 0.46 cm × 12.5 cm) and eluted at 1 mL/min using an aqueous acetonitrile gradient in the presence of 0.1% TFA (from 25 to 50% acetonitrile over the course of 45 min). Radioactivity profiles were recorded on-line with a Flo-one Packard radiodetector. (—) Radioactivity detection of tryptic digests of SHBG photolabeled with [^{3}H]ANB photoreagents alone. (•••) Radioactivity detection of tryptic digests of SHBG photolabeled with [^{3}H]ANB photoreagents in the presence of a 10-fold molar excess of DHT.

The radioactive peaks which could not be abolished by photolabeling in the presence of DHT were all found to have chromatographic properties (retention times in HPLC and R_f values after TLC on silica gel) similar to those of the photolyzed products of the corresponding photoreagents. These peaks represented ~90% of the radioactivity in the case of the two inefficient [^{3}H]ANP-M and [^{3}H]ANTFP-M photoreagents. In all other cases, the amount of unbound steroids varied from 39 to 50% of the total amount of radioactive peaks, depending on the photoreagents. No further unbound radioactivity was found after a second HPLC separation of peptides photolabeled with [^{3}H]ANB-P, [^{3}H]-ANP-P, or [^{3}H]ANTFP-E. Another control was carried out by recording the HPLC radioactivity profiles as a function of the time course of trypsin hydrolysis of SHBG photolabeled with [^{3}H]ANB-P which showed that the intensity of the peak of unbound radioactivity remained unchanged, in contrast to the progressive increase in the peaks corresponding to photolabeled peptides. These results indicate that the fraction of photolyzed photoreagents, which remains adsorbed to SHBG, even after exclusion chromatography under denaturing conditions, is rapidly released during the course of trypsin hydrolysis and does not result from cleavage of covalently bound radioactivity under the acidic conditions of HPLC separations. Therefore, the presence of noncovalently bound photolyzed steroids which are not eliminated by exclusion chromatography performed on the uncleaved photolabeled SHBG is presumably the main factor account-

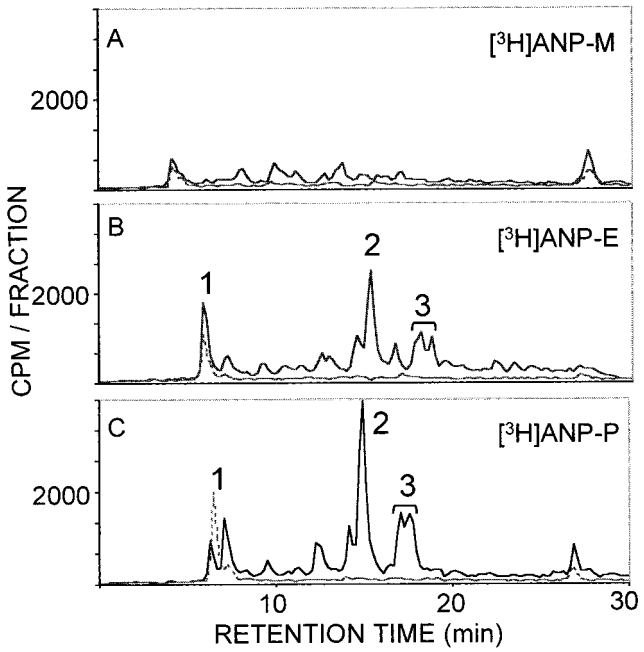

FIGURE 3: Reverse-phase HPLC separation of tryptic peptides of SHBG photolabeled with the [^{3}H]ANP photoreagents. The tryptic digests were applied on a C_{18} column (Nucleosil AB, 5 μm, 0.46 cm $\times$ 12.5 cm) and eluted at 1 mL/min using an aqueous acetonitrile gradient in the presence of 0.1% TFA (from 25 to 50% acetonitrile over the course of 45 min). Radioactivity profiles were recorded on-line with a Flo-one Packard radiodetector. (—) Radioactivity detection of tryptic digests of SHBG photolabeled with [^{3}H]ANP photoreagents alone. (···) Radioactivity detection of tryptic digests of SHBG photolabeled with [^{3}H]ANP photoreagents in the presence of a 10-fold molar excess of DHT.

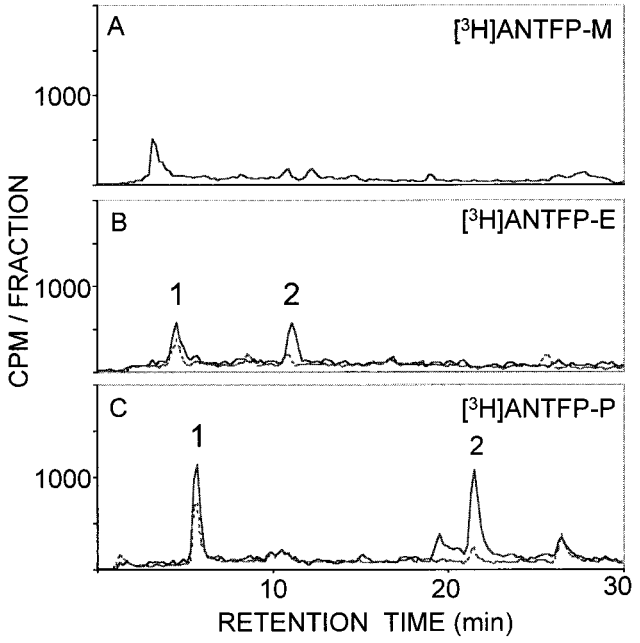

FIGURE 4: Reverse-phase HPLC separation of tryptic peptides of SHBG photolabeled with the [^{3}H]ANTFP photoreagents. The tryptic digests were applied on a C_{18} column (Nucleosil AB, 5 μm, 0.46 cm $\times$ 12.5 cm) and eluted at 1 mL/min using an aqueous acetonitrile gradient in the presence of 0.1% TFA (from 25 to 50% acetonitrile over the course of 45 min). Radioactivity profiles were recorded on-line with a Flo-one Packard radiodetector. (—) Radioactivity detection of tryptic digests of SHBG photolabeled with [^{3}H]ANTFP photoreagents alone. (···) Radioactivity detection of tryptic digests of SHBG photolabeled with [^{3}H]ANTFP photoreagents in the presence of a 10-fold molar excess of DHT.

ing for the apparent higher levels of specific covalent attachment as compared with those observed after photoinactivation.

Photolabeling of SHBG with [^{3}H]ANB-M or [^{3}H]ANB-P in the presence of 15 mM glutathione or 4-aminobenzoate, used as scavengers (*27*), had no effects on the radioactivity profiles of tryptic peptides as compared with photolabeling in PBS alone. Furthermore, control experiments carried out with tryptic peptides after photolabeling of heat-denatured SHBG with [^{3}H]ANB-M or [^{3}H]ANB-P revealed no radioactive peaks at the expected HPLC retention times.

Immunopurification of Photoaffinity-Labeled Peptides. The preparative separation of radioactive peptides from tryptic digests of SHBG photolabeled with each radioactive photoreagent was realized after a prior immunopurification step, using immobilized polyclonal rabbit anti-testosterone antibodies selected for their high cross-reactivity with the nine 17α-substituted androstanediol photoreagents employed in this study. The mixture of retained photolabeled peptides (optimized retention yield > 85%) was eluted with an aqueous solution of dioxane, according to a previously reported protocol (*24*), with yields ranging from 50% for peptides labeled with [^{3}H]ANTFP-E and [^{3}H]ANTFP-P to 90% for peptides labeled with [^{3}H]ANB-P. The radioactivity profiles after HPLC separation of the immunopurified fraction could be superimposed on those of the corresponding crude tryptic digests and showed a good correlation with the peaks of immunopurified peptides, also detected by recording the absorbance at 220 nm (data not shown), thus demonstrating that the immunopurification step did not operate any selection among photolabeled peptides that could modify significantly radioactivity profiles.

The overall yields of preparative separations of radioactive tryptic peptides obtained from 40 nmol of SHBG, irradiated after incubation with an equimolar amount of the three [^{3}H]-ANB derivatives or of the two photoreagents ([^{3}H]ANP-E and [^{3}H]ANP-P), ranged from approximately 100 to 250 pmol of each of the photolabeled peptides. Similar experiments on 100 nmol of SHBG irradiated in the presence of [^{3}H]ANTFP-E or [^{3}H]ANTFP-P led to approximately 60 or 100 pmol of photolabeled peptide, respectively.

Edman Sequencing of Photolabeled Tryptic Peptides Corresponding to Residues 73—*94.* Edman sequencing of the major peptides photolabeled with [^{3}H]ANB-M (combined peaks 1 and 2, and isolated peak 2, in Figure 2A) and [^{3}H]-ANB-E (peak 2 in Figure 2B), as well as of the minor peptide photolabeled with [^{3}H]ANP-P (double peak 3 in Figure 3C), showed the same single sequence of residues 73—94 of SHBG (*28*) in which no known amino acid residue was identified at cycle 12 (Table 2). The major peak of radioactivity was eluted at cycle 12 in all cases, and corresponded in magnitude to the amounts of PTH derivatives measured in the preceding cycle, thus suggesting labeling of the same Trp-84 amino acid residue. Edman sequencing was also performed on the two other minor peptides photolabeled with [^{3}H]ANB-E (peaks 1 and 3 in Figure 2B) which showed the same single sequence as observed for the major peak 2, including the absence of any detectable residue at cycle 12, suggesting that Trp-84 is also the photolabeled residue.

Table 2: Amino Acid Sequence Analysis of SHBG Tryptic Peptides (Residues 73−94) Photolabeled with [^{3}H]ANB-M, [^{3}H]ANB-E, and [^{3}H]ANP-P

		[^{3}H]ANB-M peptide (peaks 1 + 2)[a] 800 000 dpm, 184 pmol[d]		[^{3}H]ANB-M peptide (peak 2)[a] 400 000 dpm, 92 pmol[d]		[^{3}H]ANB-E peptide (peak 2) [b]500 000 dpm, 115 pmol[d]		[^{3}H]ANP-P peptide (peak 3) [c]268 000 dpm, 62 pmol[d]	
cycle	amino acid	PTH derivative (pmol)	radioactivity (dpm)	PTH derivative (pmol)	radioactivity (dpm)	PTH derivative (pmol)	radioactivity (dpm)	PTH derivative (pmol)	radioactivity (dpm)
1	D	105.7	53403	43.5	12616	57.0	21286	35.1	16320
2	G	80.0	36222	45	8049	69.7	15819	33.0	8520
3	R	74.4	24204	20.3	6147	41.2	11945	28.5	7548
4	P	101.1	18342	41.4	5985	66.9	9628	31.3	9628
5	E	86.3	11955	36.9	4791	55.2	7826	25.4	3526
6	I	93.3	10527	38.4	5764	58.6	7434	29.6	7434
7	Q	86.0	9771	34.5	5564	56.7	6013	28.0	3278
8	L	90.2	8394	37.8	4885	58.3	5957	29.6	2856
9	H	45.3	9930	18.0	5761	29.2	5527	18.6	3122
10	N	61.2	12543	28.4	6636	42.5	6751	24.2	4508
11	H	22.7	33705	8.5	14570	13.5	21045	7.5	10388
12	(W)	(22.8)[e]	99027	(5.8)[e]	27107	(11.2)[e]	48577	(5.2)[e]	22644
13	A	44.5	68757	18.6	18704	27.8	32714	18.5	12388
14	Q	40.1	44964	15.8	13870	26.1	17846	15.4	6066
15	L	33.8	29658	14.1	11536	21.5	14840	13.0	4844
16	T	10.6	25710	6.1	9019	6.2	11645	3.2	3220
17	V	20.8	18789	10.4	7754	13.8	8645	6.1	2342
filter			260000		118046		115000		66797

[a] Peptides 1 and 2 (unseparated mixture) and isolated peptide 2 in Figure 2A. [b] Peptide 2 in Figure 2B. [c] Peptide 3 in Figure 3C. [d] Picomoles of labeled peptide applied to the sequencer, calculated from the specific activity of the photoreagent. [e] Picomoles of amino acid estimated from the amount of radioactivity eluted at cycle 12.

These four photolabeled peptides showed also a significant increase in the amount of radioactivity at the level of Edman cycle 11 which could represent a partial labeling of the corresponding His-83 residue recovered in rather low yield in all cases. To examine such a hypothesis, complementary sequencing experiments were performed on shorter subcleaved peptides. For SHBG photolabeled with [^{3}H]-ANB-M, some of the first experiments of trypsin hydrolysis were found to afford two sequences of residues 82−94 homologous to those corresponding to peaks 1 and 2, exhibiting a similar labeling of Trp-84 (*29*). For SHBG photolabeled with [^{3}H]ANB-E, the major peptide (peak 2) was subcleaved by elastase which led to the sequence of residues 82−87 (N-H-X*-A-Q-L) in which no Trp-84 could be identified at the third Edman cycle. For these three subcleaved peptides, the major peak of radioactivity was released at the level of Trp-84 but no radioactive peak was eluted at the level of His-83, thus ruling out the above-mentioned hypothesis of a partial labeling of this residue. However, it should be noted that the cleavage of the peptidic bond between His-81 and Asn-82 is unusual. This unexpected site of subcleavage observed with both trypsin and elastase enzymes may derive from yet undetermined factors such as partial photodegradation of the protein and/or the presence of the photolabel.

Edman Sequencing of Photolabeled Tryptic Peptides Corresponding to Residues 126−134 and 126−135. Edman sequencing of the peptide photolabeled with [^{3}H]ANB-E (peak 3′, retention time shown in Figure 2B) and of the two peptides photolabeled with [^{3}H]ANB-P (peaks 1 and 2 in Figure 2C) identified PTH derivatives up to cycles 8, 6, and 4, respectively, all corresponding to the N-terminal amino acids of the tryptic peptide composed of residues 126−134 (Table 3). The absence of PTH derivatives identified at cycle 5 corresponding to Pro-130 and the dramatic decrease in the yields of PTH amino acids detected after cycle 5, in the first case, or their total absence, in the last case, suggested a covalent attachment of the photoreagents to Pro-130. However, in all cases, no radioactive peak was measured at cycle 5, but the major radioactive peak was observed at the first cycle while large amounts of radioactivity were still released during the next three cycles. Furthermore, only 12−26% of the radioactivity was recovered in the PTH effluents; on the other hand, 4−5% of the radioactivity remained on the filter, and 69−84% was presumably lost in the washes. Such a distribution of radioactivity points to the hypothesis of a labile covalent attachment of the photoreagents to Pro-130 which has been shown above to resist slightly acidic HPLC conditions (0.1% TFA) but is probably readily hydrolyzed during Edman degradation, after treatment with trifluoroacetic acid, and released in the wash steps. Indeed, a control experiment, carried out by adding 25% trifluoroacetic acid to solutions of the two separated tryptic peptides photolabeled with [^{3}H]ANB-P, was found to dissociate the tritiated steroid from the peptides within 1 h at 25 °C. The Edman sequence of the radioactive peptide photolabeled with [^{3}H]ANB-P corresponding to peak 1 was contaminated by a minor amount (∼10%) of the peptide fragment corresponding to residues 73−94 which was sequenced up to the Leu-87 residue (data no shown). This minor photolabeled peptide was presumably photolabeled at the level of Trp-84 since no PTH derivative of this residue could be detected.

Edman sequencing of the five radioactive tryptic peptides photolabeled with [^{3}H]ANP-E (peak 2 and double peak 3 in Figure 3B), [^{3}H]ANP-P (peak 2 in Figure 3C), [^{3}H]-ANTFP-E (peak 2 in Figure 4B), or [^{3}H]ANTFP-P (peak 2 in Figure 4C) showed in all cases the same sequence corresponding to the tryptic peptide composed of residues 126−135, although the last Arg residue of the minor peptide (double peak 3) photolabeled with [^{3}H]ANP-E could not be

Table 3: Partial Amino Acid Sequence Analysis of SHBG Tryptic Peptides (Residues 126−134) Photolabeled with [^{3}H]ANB-E and [^{3}H]ANB-P

		[^{3}H]ANB-E peptide (peak 3′)[a] 900 000 dpm, 170 pmol[c]		[^{3}H]ANB-P peptide (peak 1)[b] 400 000 dpm, 90 pmol[c]		[^{3}H]ANB-P peptide (peak 2)[b] 700 000 dpm, 150 pmol[c]	
cycle	amino acid	PTH derivative (pmol)	radioactivity (dpm)	PTH derivative (pmol)	radioactivity (dpm)	PTH derivative (pmol)	radioactivity (dpm)
1	Q	102	90692	33.5	21596	84	32136
2	V	88	46168	13.4	17232	85.4	14676
3	S	14	23816	0.8	21880	11.9	10036
4	G	49	10720	1.1	16420	43.3	6640
5	(P)	(−)[d]	10408	(−)[d]	9256	(−)[d]	3836
6	L	4.7	14012	0.8	5896	(−)[d]	3676
7	T	0.8	6584	(−)[d]	4640	(−)[d]	2656
8	S	0.6	7012	(−)[d]	3344	(−)[d]	2216
9	(K)	(−)[d]	3724	(−)[d]	2240	(−)[d]	2748
10	(R)	(−)[d]	6376	(−)[d]	2740	(−)[d]	1996
filter			41260		19000		26000

[a] Peptide 3′ (retention time shown in Figure 2B). [b] Peptides 1 and 2 in Figure 2C. [c] Picomoles of labeled peptide applied to the sequencer, calculated from the specific activity of the photoreagent. [d] PTH derivatives not identified.

Table 4: Amino Acid Sequence Analysis of SHBG Tryptic Peptides (Residues 126−135) Photolabeled with [^{3}H]ANP-E, [^{3}H]ANP-P, [^{3}H]ANTFP-E, and [^{3}H]ANTFP-P

		[^{3}H]ANP-E peptide (peak 2)[a] 282 000 dpm, 50 pmol[d]		[^{3}H]ANP-E peptide (peak 3)[a] 160 000 dpm, 34 pmol[d]		[^{3}H]ANP-P peptide (peak 2)[b] 700 000 dpm, 150 pmol[d]		[^{3}H]ANTFP-E peptide (peak 2)[c] 290 000 dpm, 62 pmol[d]		[^{3}H]ANTFP-P peptide (peak 2)[c] 256 000 dpm, 55 pmol[d]	
cycle	amino acid	PTH derivative (pmol)	radioactivity (dpm)	PTH derivative (pmol)	radioactivity (dpm)	PTH derivative (pmol)	radioactivity (dpm)	PTH derivative (pmol)	radioactivity (dpm)	PTH derivative (pmol)	radioactivity (dpm)
1	Q	22.2	32552	15.0	13709	77.1	16860	25.9	62121	28.6	22136
2	V	18.3	17257	12.1	9492	96.6	17275	21.2	17377	15.7	14676
3	S	1.1	20180	2.6	6926	16.2	17744	2.4	32676	0.9	8036
4	G	9.2	14440	6.7	11781	55.8	16530	11.0	16453	10.8	7880
5	P	9.4	9950	6.3	16485	50.4	12914	10.8	12491	11.5	12925
6	L	10.2	10225	6.4	11410	49.1	14012	13.7	10115	10.4	9800
7	T	3.3	10824	1.9	11410	17.2	12000	3.5	8886	3.8	7680
8	S	1.7	9780	0.9	9493	6.3	13190	1.4	8123	1.3	8825
9	K	(8.4)[e]	39735	0.4	21889	(7.5)[e]	35100	1.4	28798	1.2	22870
10	R	1.4	19544		10944	3.6	32250	0.9	25942	1.1	29020
filter			72750		19800		67000		39000		26000

[a] Peptides 2 and 3 in Figure 3B. [b] Peptide 2 in Figure 4C. [c] Peptides 2 in panels B and C of Figure 4. [d] Picomoles of labeled peptide applied to the sequencer calculated from the specific activity of the photoreagent. [e] Picomoles of amino acid estimated from the amount of radioactivity that eluted at cycle 9.

detected, presumably because of the small amount of this peptide (Table 4). The Edman sequence of peptides photolabeled with [^{3}H]ANP-E (peak 2) and [^{3}H]ANP-P (peak 2) showed a total absence of Lys-134 at cycle 9, whereas a small amount of PTH derivative of Lys-134 was still present for the three other peptides. In all cases, a significant peak of radioactivity was recovered at cycle 9, corresponding in magnitude to the amount of PTH of the modified lysine derivative that could be expected at this cycle from the measurements made at the preceding cycles, taking into account the expected low recovery of Ser-133 and Thr-132. The presence, in three peptides, of small amounts of the PTH derivative of Lys-134 may result from a partially labile character of the covalent attachment of the corresponding ANP-E, ANTFP-E, or ANTFP-P photoreagent to Lys-134, leading to partial cleavage during the course of HPLC purifications, and/or from a minor fraction of labeling on another amino acid residue of the same peptide.

Mass Spectrometry of the Photolabeled Tryptic Peptides Corresponding to Residues 73−94. The electrospray mass spectrum of the sequenced major peptide (residues 73−94) photolabeled with [^{3}H]ANB-M (isolated peak 1 in Figure 2A) showed two main tetravalent and trivalent ions at *m*/*z* 736.2 and 981.2, respectively, corresponding to a measured mass of 2940.7 ± 0.1 Da, whereas the average mass calculated for the covalent attachment of the nitrene derivative of the ANB-M photoreagent is only 2936.3 Da. The resulting mass increment (+4.4) was postulated to correspond to the formation of a dehydrated $Na^+ - H_2O$ adduct. The presence of an additional small peak at 731.7 (measured mass of 2922.8 Da) was assigned to a further dehydrated $Na^+ - 2H_2O$ adduct. These dehydrated ions might result from dehydration of androstanediol and possibly of the peptide, because of the presence of a threonine residue.

The second sequenced peptide (residues 73−94) photolabeled with [^{3}H]ANB-M (isolated peak 2 in Figure 2A) was analyzed by MALDI-TOF-MS, since electrospray mass spectra showed only multicharged ions leading to an overestimated measured mass with an unexplained mass increment of +14.5. The MALDI-TOF mass spectrum (linear mode) showed a major $[M + H]^+$ ion at 2938.0 Da, which is in agreement with the mass of 2936.3 Da, calculated for

the covalent attachment of 1 mol of the nitrene form of the ANB-M photoreagent. Nevertheless, a less intense signal was also observed at 2952.5 Da which corresponds to the mass increment of +14.5, found in electrospray mass spectra.

The major peptide (residues 73−94) photolabeled with [^{3}H]ANB-E (major peak 2 in Figure 2B) was analyzed by MALDI-TOF mass spectrometry since electrospray mass spectra also exhibited a mass increment of +14.5. The MALDI-TOF mass spectrum (reflector mode) exhibited a major $[M + H]^+$ ion at 2951.3 Da, which is in agreement with the average mass of 2950.4 Da, calculated for the covalent attachment of 1 mol of ANB-E photoreagent. In this case, no intense signal corresponding to the mass increment of +14.5 was observed.

The electrospray mass spectrum of the minor peptide (residues 73−94) photolabeled with [^{3}H]ANB-E (minor peak 3 in Figure 2B) exhibited a major $[M + 3H]^{3+}$ ion at 984.6 and a small $[M + 2H]^{2+}$ ion at 1476.2, corresponding to a measured mass of 2950.8 ± 0.4 Da, in agreement with the covalent attachment of 1 mol of the ANB-E photoreagent.

On the other hand, the electrospray mass spectrum of the peptide (residues 73−94) photolabeled with [^{3}H]ANP-P (double peak 3 in Figure 3C) exhibited two major $[M + 5H]^{5+}$ and $[M + 4H]^{4+}$ ions at 588.4 and 735.1, respectively, and a much weaker $[M + 3H]^{3+}$ ion at 979.8, corresponding to a measured mass of 2936.6 Da, in agreement with the average mass of 2936.4 Da, calculated for the covalent attachment of 1 mol of the nitrene form of the ANP-P photoreagent.

Mass Spectrometry of the Photolabeled Tryptic Peptides Corresponding to Residues 126−134 and 126−135. The electrospray mass spectrum of peptidic material photolabeled with [^{3}H]ANB-P, corresponding to peak 1 (Figure 2C), confirmed the presence of a mixture of two photolabeled peptides. A very weak $[M + H]^+$ ion peak at 1428.2 and a rather intense divalent ion peak at 705.9, corresponding to measured masses of 1427.2 and 1409.8 Da, respectively, are in agreement with the addition of the intact or dehydrated forms of the peptide fragment composed of residues 126−134 photolabeled with the nitrene derivative of ANB-P (calculated average masses of 1427.7 and 1409.7 Da, respectively). On the other hand, the major tetravalent ion at 738.7 and a minor trivalent ion at 990.6 (measured masses of 2950.8 and 2968.8 Da, respectively) were assigned to sodium adducts to bis- and monodehydrated forms of the peptide fragment composed of residues 73−94 covalently labeled with 1 mole of [^{3}H]ANB-P (calculated average masses of 2950.4 and 2968.4 Da, respectively). It should be noted that the photolabeled peptide corresponding to residues 73−94, although showing the most intense ion at 738.7 in the preceding mass spectrum, has been identified as only a minor side product of the photolabeled peptide corresponding to residues 126−134, by Edman sequencing of the same sample as the one analyzed by mass spectrometry. The mass spectrum of the second peptide photolabeled with [^{3}H]-ANB-P (peak 2 in Figure 2C) showed a small $[M + H]^+$ ion at 1428.2 (measured mass of 1427.2 Da) and a major divalent ion at 705.8 (measured mass of 1409.6 Da) which correspond to intact and dehydrated forms, respectively, of the peptide fragment composed of residues 126−134 covalently labeled with 1 mol of ANB-P.

The two sequenced peptides photolabeled with [^{3}H]-ANP-E (peaks 2 and 3 in Figure 3B) failed to give any interpretable mass spectra using either electrospray or MALDI-TOF techniques.

The major sequenced peptide (residues 126−135) photolabeled with [^{3}H]ANP-P (peak 2 in Figure 3C) could be analyzed by MALDI-TOF mass spectrometry in both normal and PSD modes. The mass spectrum recorded in the reflector mode showed a prominent group of peaks containing an intense signal at 1519.0, assigned to the $[M - 2H_2O + H]^+$ ion, in agreement with the isotopic mass of 1519.9 Da calculated for the bis-dehydrated $[M - 2H_2O + H]^+$ ion after covalent attachment of the nitrene derivative of ANP-P to the tryptic fragment composed of residues 126−135 of human SHBG. Other peaks were also observed, including the base peak at 1522.0, and several other lower-intensity signals, for which no unequivocal interpretation could be found, except for the rather intense peak at 1189.8, which was postulated to correspond to the monodehydrated $[M - H_2O + H]^+$ ion of the photolabeled peptide composed of residues 126−135, resulting from a cleavage of the covalently bound photolabel between the nitrophenyl ring of the chromophore and the propylamino side chain of the ANP-P photoreagent (calculated isotopic mass of 1189.9 Da). The difference found between the two observed masses at 1519.0 and 1189.8 Da, taking into account the difference in the degree of hydration of these two peaks, corresponds to 347.2 Da (329.2 + 18), representing exactly the loss of the 17α-(propylamino)androstanediol moiety replaced with a hydrogen atom (−347.3). This hypothesis was confirmed by the PSD fragment ion spectrum of the $[M - 2H_2O + H]^+$ ion, observed at 1519.4 in the PSD mode, which showed also an intense peak at an observed mass of 1191.0 Da, in keeping with the mass of 1189.8 Da found above for the minor ion present in the reflector mode spectrum. Moreover, the formation of this major monodehydrated ion from a bis-dehydrated $[M - 2H_2O + H]^+$ ion, following the loss of the 17α-(propylamino)androstanediol moiety, suggests that the second dehydration of the latter ion probably results from the androstanediol part of the photoadduct. The comparison of the PSD fragment ion spectra recorded in parallel for these two ions (Figure 5) showed several homologous a, b, and y fragment ions, especially for the first four N-terminal residues (a1, a2, a4, b2, b3, b4, y7, and y8), but also in the C-terminal region (b6, b9, and y1) which confirmed the presence of the same peptide sequence. Furthermore, b/y ion correspondences were observed for the b2/y8, b3/y7, and b9/y1 ion pairs, in both PSD spectra, whereas the b1/y9, b4/y6, b6/y4, and b7/y3 ion pairs were found only in the PSD spectrum of the 1191.0 ion. Although no b8/y2 ion pair, corresponding to a cleavage at the N-terminus of the Lys−steroid adduct, could be found, the remaining data provided by these two PSD spectra, including the presence of at least one fragment ion for all expected peptidic bond cleavages, are fully consistent with the covalent labeling of Lys-134 by [^{3}H]-ANP-P, established above by Edman sequencing.

DISCUSSION

The purpose of this study was to characterize amino acid residues in the proximity of the steroid-binding site of human SHBG by photoaffinity labeling with steroid photoreagents bearing photoactivatable aryl azide chromophores introduced

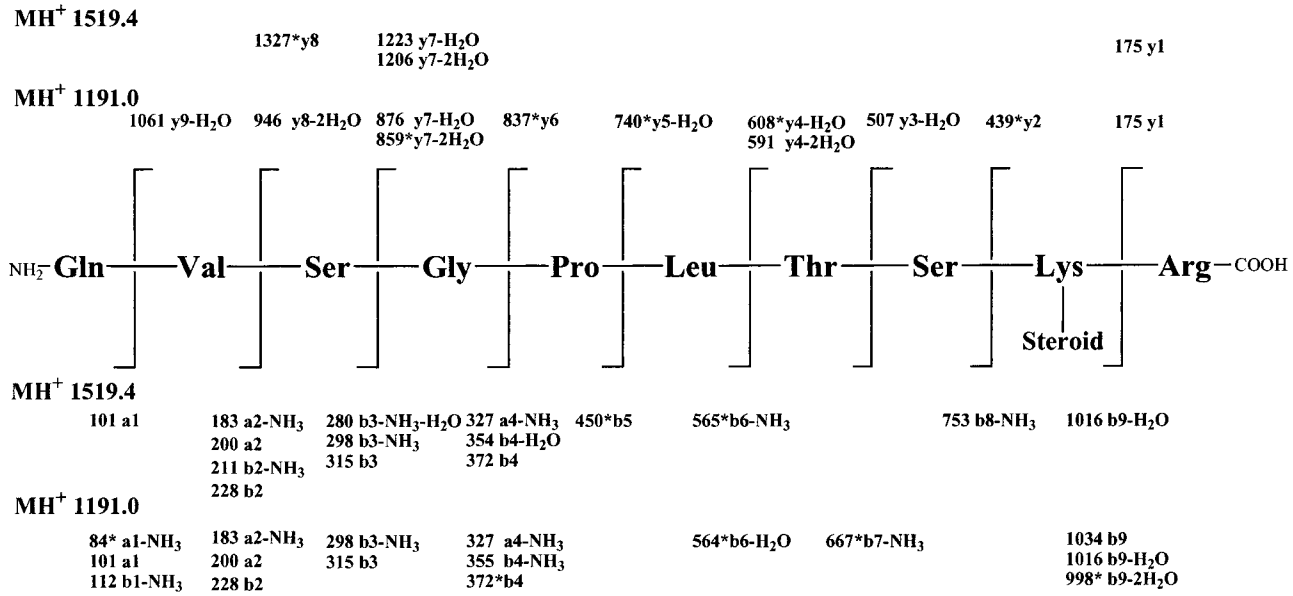

FIGURE 5: Fragmentation scheme corresponding to the PSD-MALDI-TOF mass spectra of the peptide (residues 126−135) photolabeled with [^{3}H]ANP-P (double peak 3 in Figure 3C) recorded on the bis-dehydrated $[M - 2H_2O + H]^+$ ion at 1519.4, and on its subcleaved fragment at 1191.0, attributed to the loss of the 17α-aminopropyl steroid. Asterisks denote weak fragment ion signals.

at the extremity of 17α-(aminoalkyl)-5α-androstane-3β,17β-diol precursors. These 17α-substituted steroid photoreagents should be free to enter into the binding site where the steroid may also interact through hydrogen bonding with the tertiary 17β-OH group, whereas the free extremity of the side chain may lie more or less outside of the binding site and possibly of the protein. Therefore, three intermediate aminomethyl, aminoethyl, and aminopropyl linkers having different lengths, flexibilities, and hydrophobicities were introduced between the steroid skeleton and the chromophore to increase the probability of an interaction between the chromophore and the protein at the most proximate potential amino acid targets surrounding the D ring, without impairing the correct positioning of the steroid in the binding site. Moreover, these differences were combined with the significant structural differences existing between the three ANB, ANP, and ANTFP (*26*) chromophores, thus leading to nine photoreagents.

The nine photoreagents exhibited high binding affinities for SHBG. In all cases, the relative binding affinities decreased whereas photoinactivation and photolabeling efficiencies increased when the length of the intermediate aminoalkyl linker between the steroid and the chromophore was increased or when the chromophores were changed from ANTFP to ANP and ANB for the same aminoalkyl linker. Photolabeling of the binding site of SHBG was successful with seven of the nine tested photoreagents but not with the two shortest ANP-M and ANTFP-M derivatives, whereas the two longest ANB-P and ANP-P derivatives led to the highest yields. In this study, using exclusively wavelengths of >300 nm, photoinactivation and photolabeling yields were lower with ANTFP photoreagents than with the corresponding ANB and ANP photoreagents.

The high affinity of the nine photoreagents for SHBG and the use of a stoichiometric amount of photoreagent both limit the possibility of diffusion of the photoreagent outside the binding site before photolabeling. On the other hand, the site-specific character of photoaffinity labeling of SHBG is shown by the almost total inhibition of photolabeling in the presence of an excess of DHT, which also indicates that the presence of the steroid part of the photoreagent in the binding site is required for an appropriate positioning of the photoactivatable chromophore during irradiation, although a contribution of the stacking of chromophores to potential amino acid targets cannot be ruled out as a factor increasing overall binding affinity.

Amino acid sequence analysis of isolated photolabeled tryptic fragments revealed that the radioactivity was present either on a peptide comprising residues 73−94, at the level of Trp-84 (ANB-M, ANB-E, ANB-P, and ANP-P photoreagents), or on one of the two overlapping sequences of residues 126−134, at the level of Pro-130 (ANB-E and ANB-P photoreagents), or residues 126−135, at the level of Lys-134 (ANP-E, ANP-P, ANTFP-E, and ANTFP-P photoreagents). The radioactivity corresponding to the photolabeling of the peptide composed of residues 73−94 with the three [^{3}H]ANB-M, [^{3}H]ANB-E, and [^{3}H]ANP-P derivatives was distributed among several HPLC fractions at different retention times, including double peaks, unambiguously characterized by Edman sequencing. The heterogeneity of these fractions could be partially characterized for peaks 2, corresponding to the peptides composed of residues 73−94 photolabeled with ANB-M or ANB-E photoreagents, which showed a weak UV signal at 340 nm and similar M + 14.5 ions in electrospray mass spectra, not observed for other peaks, including the isolated shoulders behind peaks 2. This unexplained M + 14.5 ion was also present as a significant contaminating signal in the MALDI-TOF mass spectrum of the peptide photolabeled with ANB-M, but not in the case of the same peptide photolabeled with ANB-E. The second site of photolabeling with [^{3}H]ANB-E (peak 3′) and [^{3}H]ANB-P derivatives (peaks 1 and 2) was tentatively localized at the level of Pro-130. The covalent character of this labile labeling could be confirmed by mass spectrometry which revealed that the two peptides (peaks 1 and 2) photolabeled with [^{3}H]ANB-P correspond to photolabeled

fragments (residues 126−134) of the same length, suggesting therefore a structural difference possibly due to an initial heterogeneity of photolabeling mechanisms and/or to modifications during sample treatments.

The photolabeling with the four [^{3}H]ANP-E, [^{3}H]ANP-P, [^{3}H]ANTFP-E, and [^{3}H]ANTFP-P derivatives was recovered predominantly at the level of Lys-134 on photolabeled peptides composed of residues 126−135 (major single peaks 2), as shown by Edman sequencing. The presence of a low yield of the PTH derivative of Lys-134 for the minor peptide photolabeled with ANP-E (minor peak 3) and for the two major peptides photolabeled with ANTFP-E or ANTFP-P (peaks 2) may also reflect a heterogeneous photolabeling leading to a partially labile covalent labeling restoring a small amount of the intact lysine residue, although other sites of labile labeling cannot be ruled out in the absence of mass spectrometric studies. However, the stable labeling of Lys-134 with the ANP-P photoreagent, leading to a total absence of Lys residue in the Edman sequence, was confirmed by mass spectrometry (PSD-MALDI-TOF-MS). It should be noted that the labile photolabeling, postulated to occur at the level of Pro-130, led to tryptic fragments beginning at Gln-126 and ending at Lys-134, whereas the unambiguously established photolabeling of Lys-134, which is expected to inhibit tryptic cleavage, led to tryptic fragments beginning at Gln-126 and ending at Arg-135. The covalent photolabeling of Lys-134 with aryl azide chromophores introduced at position 17α of steroid ligands corroborates earlier findings based on chemoaffinity labeling experiments with a 17β-bromoacetate derivative of DHT which first demonstrated the presence of Lys-134 in the vicinity of the C17 position (*8*).

A more detailed analysis of the distribution of the different covalently bound photoreagents into three different photolabeled sites (Trp-84, Pro-130, and Lys-134), according to the length of the three 17α-aminomethyl, 17α-aminoethyl, and 17α-aminopropyl intermediate linkers and to the structures of the three ANB, ANP, and ANTFP chromophores, revealed some interesting trends about factors controlling the optimal positioning of the chromophores and those resulting from different intrinsic photoreactivities. The reactivity of ANB derivatives varied from that of the short ANB-M, which labeled exclusively Trp-84, to that of the long ANB-P, which labeled predominantly Pro-130 and very slightly Trp-84, whereas ANB-E of intermediate size labeled predominantly either Trp-84 or Pro-130, according to experiments, despite apparently identical conditions. These results suggest that Trp-84 is closer to the C17 position of the steroid than Pro-130. The reactivity of ANP analogues varied from that of the short ANP-M, which failed to give any significant photolabeling, to that of the long ANP-P, which labeled simultaneously Lys-134, as the major site, and Trp-84, as the minor site, whereas ANP-E, of intermediate size, labeled exclusively Lys-134. The absence of reactivity of ANP-M toward Trp-84 may not result from an exceedingly short distance between the C17 position of the steroid and the azide function since the reactive ANB-M analogue exhibits a similar overall length. Moreover, the possibility of a lack of an appropriate intrinsic photoreactivity of the ANP chromophore was also ruled out since the long ANP-P derivative labeled Trp-84 with a yield higher than that observed with the corresponding ANB-P analogue. Therefore, the labeling of Trp-84 appears to be strongly dependent on stereochemical factors, only fulfilled by the short ANB-M and ANB-E photoreagents. Surprisingly, the long aminopropyl linkers orient ANB and ANP chromophores toward Pro-130 and Lys-134, respectively, suggesting that these two rather distant residues are equally accessible, since the overall lengths of the two photoreagents are almost identical. These two residues probably represent preferential target sites corresponding to differences in the intrinsic photoreactivities of ANB and ANP chromophores, as confirmed by the similar differences found for the shorter ANB-E and ANP-E photoreagents. The reactivity of ANTFP analogues was either undetectable, for the short ANTFP-M, or led to the exclusive labeling of Lys-134, for the two ANTFP-E and ANTFP-P derivatives, thus suggesting a photoreactivity similar to that of ANP derivatives, despite the shorter overall length of ANTFP photoreagents. Therefore, the positioning of ANP and ANTFP photoreagents does not appear to be a critical factor for the photolabeling of Lys-134, possibly because of the flexibility of lysine side chains as also suggested by the alkylation of the same Lys-134 with a 17β-bromoacetoxy derivative of DHT (*8*).

Since isomerization of singlet fluoroaryl azides to electrophilic dehydroazepine species is much less favored than for nonfluorinated analogues, the similar reactivities of ANP and ANTFP photoreagents with Lys-134 might be explained by triplet nitrene reactivity rather than by the formation of azepine, which is not favored with lysine and should lead to highly labile labeling (*30*). One may only speculate whether the labile photolabeling postulated at the level of Pro-130 can be explained by a similar triplet nitrene reactivity, since the absence of effects of glutathione or 4-aminobenzoate quenchers with the ANB-P photoreagent cannot unambiguously rule out the presence of immobilized reactive dehydroazepine intermediates, because of the possibility that quenchers may not be able to penetrate the occupied binding site. It is interesting to note that the conserved single Tyr-57 residue of human SHBG, located in the vicinity of the steroid-binding site (*15*, *19*), was not photolabeled by any of the nine photoreagents tested in this study, which rather interacted with Trp-84, or with Pro-130 and Lys-134, despite the often reported preferred reactivity of aryl azides with tyrosine residues (*30*).

Recently, while this study was in progress, the three-dimensional structure of the recombinant N-terminal domain spanning residues 1−205 of human SHBG was published (*19*). In this model, the presence of hydrogen bonds between the hydroxyl group at C17 and the conserved Asp-65 and Asn-82 residues is fully consistent with the conclusion from this study showing that the conserved Trp-84 residue must be very close to the C17 position, because of its selective photolabeling with ANB-M, the shortest of the seven effective photoreagents. On the other hand, the nonconserved photolabeled Pro-130 and Lys-134 amino acids are located in the disordered loop segment spanning residues 130−135 which was suggested to form a lid over the binding site and may influence the accessibility of these residues, according to the structures of ANB, ANP, and ANTFP photoaffinity reagents introduced in this work at the C17 position as well as to the significantly different structure of the previously reported 17β-bromoacetoxy derivative of DHT (*8*). Conversely, the absence of photolabeling with the two other short

ANP-M and ANTFP-M photoreagents may reflect either the absence of a proximal amino acid target that is sufficiently reactive with these two aryl azides (*30*) or a preferred orientation of the azide group of the chromophore toward the solvent, as expected from the orientation of the 17β-OH group of the steroid near the surface of the protein (*7*, *19*).

The good correlation between the results of photolabeling studies carried out in solution on the entire protein and the structural data obtained independently from radiocrystallographic studies supports the conclusion, otherwise established mainly from binding data, that the truncated N-terminal domain is a valid model of the steroid-binding site. Although such a conclusion implies that the C-terminal fragment has no detectable influence on the steroid binding properties of human SHBG, slight modifications of the overall rigidity of the binding site or of the mobility of some amino acid side chains, which could potentially be revealed by further comparative photoaffinity labeling studies, cannot be ruled out.

ACKNOWLEDGMENT

We are particularly indebted to M. Courteau, D. Mazzocut, and L. Denoroy (IBCP-CNRS, Lyon, France) for sequence determinations and to M. Becchi and M. M. Flament (Centre Commun de Spectrométrie de Masse, CNRS, Lyon-Solaize, France) for mass spectra. Thanks are also due to M. Ainouze for technical assistance and to J. Carew for help in editing the manuscript.

SUPPORTING INFORMATION AVAILABLE

Figures showing the time course of photolysis of ANB-M, ANP-M, and ANTFP-P photoreagents, Scatchard plots of ANB photoreagents, NaDodSO_4−polyacrylamide gel electrophoresis of photolabeled CNBr peptides, the additional Edman sequences of minor and subcleaved photolabeled peptides, and mass spectra of photolabeled peptides. This material is available free of charge via the Internet at htpp://pubs.acs.org.

REFERENCES

1. Hammond, G. L. (1990) *Endocr. Rev. 11*, 80−91.
2. Petra, P. H. (1991) *J. Steroid Biochem. Mol. Biol. 40*, 735−753.
3. Westphal, U. (1986) in *Steroid Protein Interactions II. Monographs in Endocrinology*, Vol. 27, Springer-Verlag, New York.
4. Avvakumov, G. V., Muller, Y. A., and Hammond, G. L. (2000) *J. Biol. Chem. 275*, 25920−25925.
5. Grenot, C., de Montard, A., Blachère, T., Mappus, E., and Cuilleron, C. Y. (1988) *C. R. Seances Acad. Sci., Ser. 3 307*, 391−396.
6. Grenot, C., de Montard, A., Blachère, T., Rolland de Ravel, M., Mappus, E., and Cuilleron, C. Y. (1992) *Biochemistry 31*, 7609−7621.
7. Kassab, D., Pichat, S., Chambon, C., Blachère, T., Rolland de Ravel, M., Mappus, E., Grenot, C., and Cuilleron, C. Y. (1998) *Biochemistry 37*, 14088−14097.
8. Namkung, P. C., Kumar, S., Walsh, K. A., and Petra, P. H. (1990) *J. Biol. Chem. 265*, 18345−18350.
9. Danzo, B. J., Parrott, J. A., and Skinner, M. K. (1991) *Endocrinology 129*, 690−696.
10. Bocchinfuso, W. P., Warmels-Rodenhiser, S., and Hammond, G. L. (1992) *FEBS Lett. 301*, 227−230.
11. Joseph, D. R., and Lawrence, W. (1993) *Mol. Endocrinol. 7*, 488−496.
12. Sui, L., Cheung, A. W. C., Namkung, P. C., and Pétra, P. H. (1992) *FEBS Lett. 310*, 115−118.
13. Bocchinfuso, W. P., and Hammond, G. L. (1994) *Biochemistry 33*, 10622−10629.
14. Danzo, B. J., and Joseph, D. R. (1994) *Endocrinology 135*, 157−167.
15. Pétra, P. H., Woodcock, K. T., Orr, W. R., Nguyen, D. K., and Sui, L. (2000*) J. Steroid Biochem. Mol. Biol. 75*, 139−145.
16. Suzuki, Y., Itagaki, E., Mori, H., and Hosoya, T. (1977) *J. Biochem. 81*, 1721−1731.
17. Musto, N. A., Gunsalus, G. L., Milijkovic, M., and Bardin, C. W. (1977) *Endocr. Res. Commun. 4*, 147−157.
18. Hildebrand, C., Bocchinfuso, W. P., Dales, D., and Hammond, G. L. (1995) *Biochemistry 34*, 3231−3238.
19. Grishkovskaya, I., Avvakumov, G. V., Sklenar, G., Dales, D., Hammond, G. L., and Muller, Y. A. (2000) *EMBO J. 19*, 504−512.
20. Cunningham, G. R., Tindall, D. J., Lobl, T. J., Campbell, J. A., and Means, A. R. (1981) *Steroids 38*, 243−262.
21. Mappus, E., Chambon, C., Fenet, B., Rolland de Ravel, M., Grenot, C., and Cuilleron, C. Y. (2000) *Steroids 65*, 459−481.
22. Taylor, C. A., Jr., Smith, H. E., and Danzo, B. J. (1980) *Proc. Natl. Acad. Sci. U.S.A. 77*, 234−238.
23. Grenot, C., and Cuilleron, C. Y. (1979) *Steroids 34*, 15−34.
24. Rousselot, P., Mappus, E., Blachère, T., Rolland de Ravel, M., Grenot, C., Tonnelle, C., and Cuilleron, C. Y. (1997) *Biochemistry 36*, 7860−7868.
25. Schägger, H., and von Jagow, G. (1987) *Anal. Biochem. 166*, 368−379.
26. Soundararajan, N., and Platz, M. S. (1990) *J. Org. Chem. 55*, 2034−2044.
27. Bayley, H. (1983) in *Photogenerated Reagents in Biochemistry and in Molecular Biology* (Work, T. S., and Burdor, R. H., Eds.) pp 107−111, Elsevier, Amsterdam.
28. Walsh, K. A., Titani, K., Takio, K., Kumar, S., Hayes, R., and Petra, P. H. (1986) *Biochemistry 25*, 7584−7590.
29. Chambon, C. (1997) Ph.D. Thesis, Université Claude Bernard, Lyon, France.
30. Kotzyba-Hibert, F., Kapfer, I., and Goeldner, M. (2000) *Angew. Chem., Int. Ed. 34*, 1296−1312.

BI011504S